

## The Auger Fluorescence Detector electronics

H. Gemmeke<sup>1</sup> for the Pierre Auger Observatory Collaboration<sup>2</sup>

<sup>1</sup>Department of Data-Processing and Electronics, Forschungszentrum Karlsruhe, POB 3640, 76021 Karlsruhe, Germany

<sup>2</sup>Observatorio Pierre Auger, Av. San Martin Norte 304, (5613) Malargüe, Argentina

### Abstract.

The Fluorescence Detector of Auger consists of 30 telescopes covering a field of  $30^\circ \times 30^\circ$  each with 440 photomultipliers (PMT). The high dynamic range of signals (15 bit) is managed by an active voltage divider at the PMTs, amplifiers with programmable gain and data conversion in a high and a low gain range. The DC-level of the night-sky background can be monitored by a built-in opto-coupled linear circuit or by analysis of the fluctuation of the background signal. The signal of the PMTs is sampled at a rate of 10 MHz with 12 bit resolution. A sum channel with lower gain records the high pulse contributions. A 3-level trigger system uses hardware pattern recognition to reduce the 10 MHz per pixel rate (13 200 pixel) to 0.02/s random events per telescope. The fast read-out is achieved by a PC-based LINUX system optimized for long lifetime. The design and performance of the electronics and trigger is presented together with first results of measurements.

phel/100 ns. The electronic noise of the analogue processing system should be well below this limit to allow the detection of far-out events and maximizing their detection efficiencies.

A very flexible re-programmable 2-level hardware trigger introduced by a field programmable gate array (FPGA) technique is able to reduce the 10 MHz sampling rate at each PMT down to a trigger rate far below 1 Hz for a complete mirror system. The software trigger in the mirror PC drives the read-out of the frontend electronics (see fig.1) and supplies a further reduction of data rate by a factor 50. The geometry of the electronic system in fig. 1 reflects the natural structure of the FD-detector. A 10 Mbit/s to 100 Mbit/s LAN-switch connects the 6 mirror systems of an eye to the eye PC. The eye PC is the boot device for the mirror-PCs and the last stage of storage and data processing before transfer of the data by directional radio to central data processing at Malargüe.

### 1 Introduction

The Auger Fluorescence Detector measures the tracks of cosmic showers as fluorescence of  $N_2$  molecules in the night sky in coincidence with a ground array of water-Cherenkov detectors. The energy spectrum, the arrival direction, and the lateral distribution of primary particles above  $10^{19}$ eV will be deduced by 3-D reconstruction of coincidental events (Auger design report, 1997). The field of view of  $180^\circ$  or  $360^\circ$  and  $30^\circ$  above the horizon are composed of telescopes covering a field of  $30^\circ \times 30^\circ$ . Each telescope consists of a mirror system and a camera equipped with 440 PMTs. One PMT (pixel) covers a cone of  $1.5^\circ$  in the sky. Simulations of cosmic showers in the energy range of  $10^{19}$  to  $10^{21}$  eV and at a distance range of 5 to 30 km show a dynamic range of the signals of 15 bit. The sensitivity for far-out events should be in the range of the sky background, estimated to the order of 2.7

Correspondence to: H. Gemmeke (gemmeke@hpe.fzk.de)

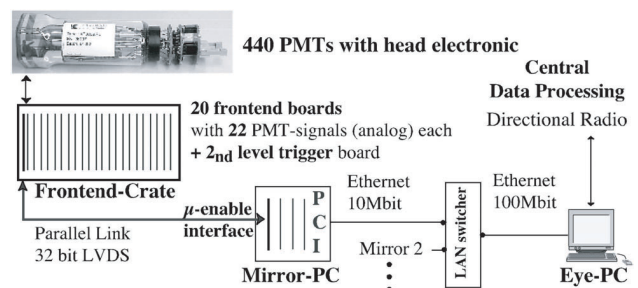


**Fig. 1.** Structure of electronics from photomultiplier via frontend crate, mirror-PC and LAN-switcher to eye-PC.

In the next three sections the present status of analogue and digital electronics, triggers and data acquisition system (DAQ) will be described. Due to the recent successful integration tests in Europe and installation and commissioning in Malargüe (Argentina) some first results could be discussed.

## 2 Analogue Processing

The analogue electronics is composed of two parts: The head electronics (HE) based on 3 boards at the PMTs (see fig. 1) and the analogue frontend boards attached to the digital first level trigger board. A distribution board in between provides routing for signals and high and low voltage power supplies.

### 2.1 Head Electronics

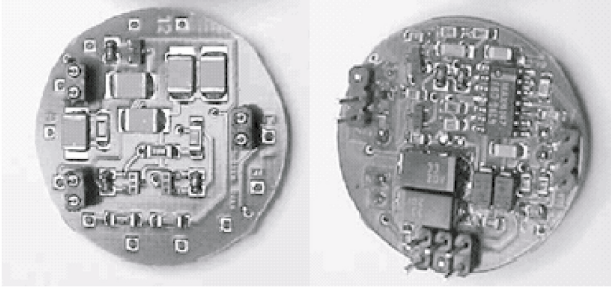


**Fig. 2.** Active voltage divider (left) and current-monitor board (right) of the head electronics.

The main function of the head electronics is to deliver with low noise and high dynamic range and at the same time low power consumption a linear output signal to the frontend board. To overcome gain stability problems with the varying background of the night sky from 2.7  $\text{phel}/100\text{ns}$  at moonless nights to a factor 30 higher values with moon present an active voltage divider was developed, fig. 2 left. That helps also in the case of star images moving slowly over the field of view. A factor 2 lower power consumption than a conventional divider design was achieved (Agiro et al. , 1999) with only 140 mA divider current.

The PMTs are AC-coupled and a direct measurement of the current at the frontend board is not possible. Therefore the DC-anode current of the PMTs are measured with the aid of a novel opto-coupled device (Camin et al. , 1999; Infineon , 2000) and added to the analogue signal of the PMT. The achieved precision of this current monitor was in the range of 0.4 nA.

### 2.2 Analogue Frontend Board

Each frontend board serves 22 channels. 20 frontend boards are necessary to cover a complete telescope with  $20 \times 22$  channels. The analogue part of the frontend board receives the signal from the head electronics and contains an amplifier with programmable gain. This allows compensation of ageing effects of the PMTs and matching the gains varying from channel to channel. That is especially necessary because of the split in a high gain direct conversion (12 bit) and a low gain sum per 11 channels. A  $3_{rd}$  order active filter with a time constant of 140 ns is installed as an anti-aliasing filter for the 10 MHz ADC. The measured noise at a PMT-gain of  $5 \cdot 10^4$  was smaller than 0.5  $\text{phel}/100\text{ns}$ , ca. 20% of the

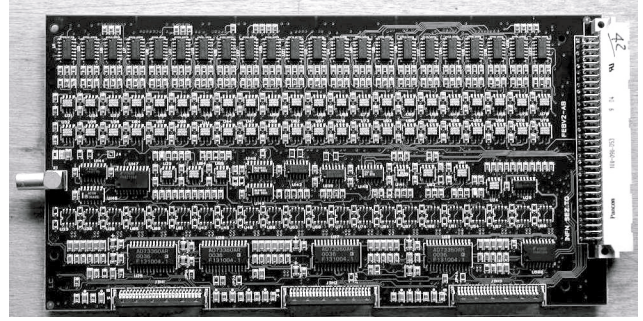


**Fig. 3.** Analogue frontend board with 22 input channels.

expected sky background. The cross-talk was smaller than  $6 \cdot 10^{-4}$ . The linearity was better than 2% without and 4% with large DC-background. All these values are better than the design goals. The quasi DC PMT current-monitor is digitized by a 16 bit  $\Sigma\Delta$ -ADC.

## 3 Digital Electronics and Trigger

The analogue frontend is readout by a 10 MHz 12 bit ADC. The ADC delivers its data directly to a 1000 samples deep 16 bit ring-buffer recording a film around the trigger. 32 different buffers per pixel are sufficient for queuing of events until the result of  $2_{nd}$  and  $3_{rd}$  level trigger validate or clear an event. All functions of the digital electronics are implemented in re-programmable FPGA logic in order to achieve high flexibility, cost-effectiveness and ease of maintenance. The high data rate from the sampling of the PMT signals is reduced through a multilevel trigger system. The  $1_{st}$  level trigger works on the sequence of pixel data in a 100 ns rhythm, while the  $2_{nd}$  level trigger analyses every microsecond the trigger picture of the first level trigger of the complete telescope (Gemmeke et al. , 2000).

### 3.1 $1_{st}$ Level Trigger by Digital Filter

The  $1_{st}$  level trigger is built by four FPGAs (Altera Flex 10k50) each controlling 6 pixels (see fig. 4). A programmable digital filter smoothes statistical fluctuations of the sky noise background out. As filter algorithm the sliding sum of the last 4 to 16 ADC-samples is used. As result the fluctuation of the input background is decreased by a factor 2 to 4. The digital first level trigger threshold is regulated to keep the trigger rate in the range of 100 to 200 Hz and to avoid the increase of background coincidences due to increasing number of background triggers. The used two-point regulation scheme is very robust and was tested with LED light sources.

Furthermore the fluctuation of the background before the digital filter is evaluated in the FPGA to yield a simple statistical current monitor:  $I \propto \sigma^2$ . First measurements show in the interesting range of inspection up to 100  $\text{phel}/100\text{ns}$  sky-background errors well below 10%.

The introduced very effective flexible FPGA hardware trig-

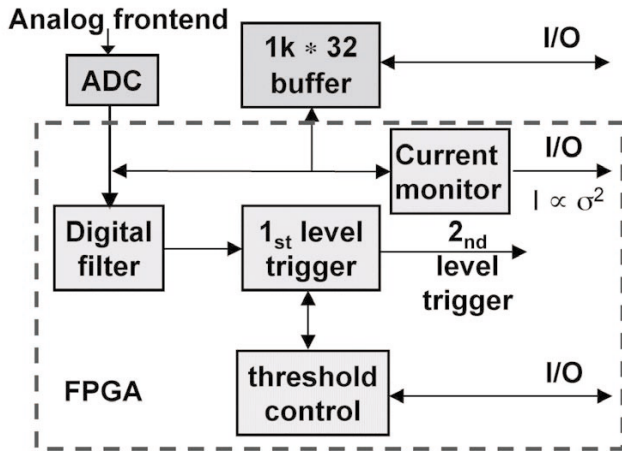


Fig. 4. Functional diagram of first level trigger for each pixel.

ger uses consequently parallel processing and thereby introduces a computing power of  $2 \cdot 10^8$  operations/s/pixel.

### 3.2 2<sub>nd</sub> Level Trigger by Track Recognition

The coincidence-time of the first level trigger signals is programmable between 1 and  $32 \mu\text{s}$ . The pixel trigger is read-out every ms and analysed using a FPGA logic (10k100 Altera FPGA). The main task of the highly parallel and pipelined logic is to recognize straight tracks in the camera image. The installed algorithm regards 5 pixels as a straight track if they are shaped like the fundamental pattern in fig.5 and those created by rotation and mirror reflections. The algorithm accepts also patterns where one pixel out of 5 is missing. This case is necessary if the touched pixel has only a peripheral sub-threshold hit or the pixel is defect. All together we got 37163 different combinations of patterns. The trigger recognition in the 2<sub>nd</sub> level trigger FPGA corresponds to an integer computing power of  $8 \cdot 10^{10}$  operations per s. This computing power together with the first level trigger was necessary to get the 10 MHz data-rate of all pixels down to 1 Hz/mirror.

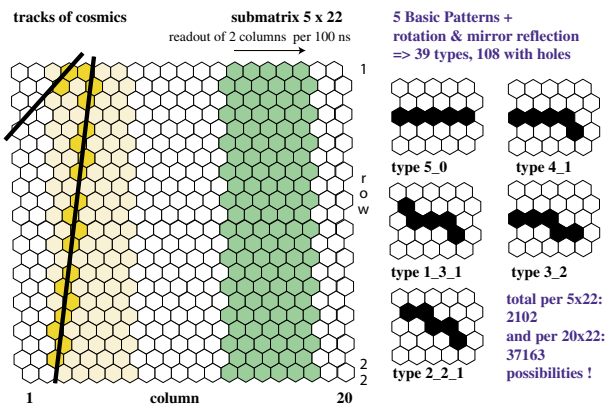


Fig. 5. Pattern recognition with the 2<sub>nd</sub> level trigger.

### 3.3 3<sub>rd</sub> Level Software Trigger

The 3<sub>rd</sub> level software trigger uses the time structure of each event and searches for two 5-pixel triggers, which combine to a trigger with minimum track length of 6 pixels.

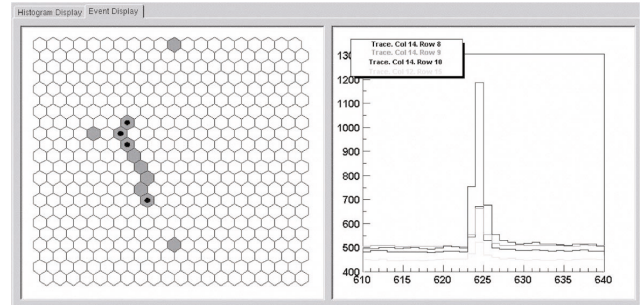


Fig. 6. Direct hit of the PMTs by a cosmic. The black marked pixels are displayed in the right spectrum. One channel corresponds to 100 ns. The track is shorter than two channels or 200 ns.

Due to simulations the time span of ultra high relativistic showers are larger than 400 ns and smaller than  $10 \mu\text{s}$ . Setting such a window on the data will reject fast Čerenkov, nearby muons and direct hits of the PMTs as shown in fig. 6. Also slow moving objects like satellites, aircrafts, planets, and stars will be rejected. The time order of consecutive pixels in a track is a further tool to recognize non-background events. All together we expect a background rate of the software trigger per mirror of lower than 0.02 Hz.

## 4 DAQ system

The read-out is based on a hierarchical architecture. At the frontend industry-PCs (mirror PC) perform the data readout and 3<sub>rd</sub>-level software trigger, see fig. 7. The mirror PCs of one eye are connected via a 10 Mbit/s - 100 Mbit/s network switch to the eye PC. The used operation system is Linux.

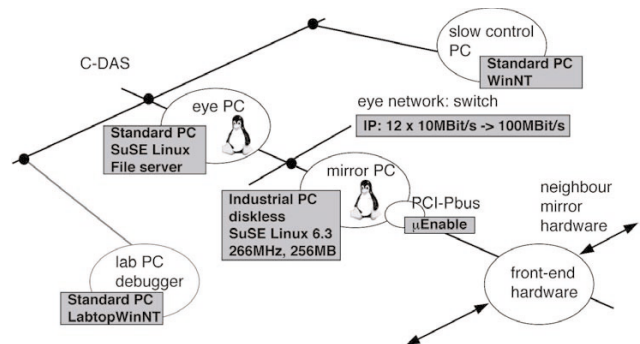
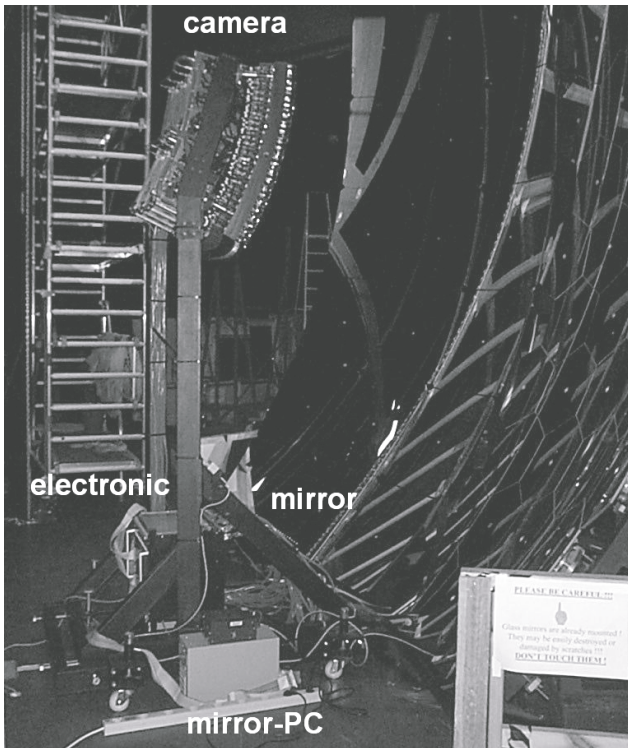


Fig. 7. Two level data acquisition system of FD.

The mirror-PC is optimized for long lifetime by using diskless PC-systems and no fans on the CPUs. Large memories (256 Mbytes) were installed to lock all necessary tasks after boot time at the mirror PC and minimize download delays

whilst data acquisition. Connection to central computing, slow control, and other computers for debugging are done through the second LAN to the eye PC protecting the data read-out from additional data traffic. The read-out software was developed with the aid of UML (unified modelling language) under C++. The integration of monitoring, slow-control and histogramming is based on software packages like ROOT, CORBA, and OPC.

## 5 Present Status and Summary



**Fig. 8.** First installed telescope with mirror, camera, and electronics in Los Leones, Malargüe.

The first telescope with electronics is successfully running in Malargüe since end of May 2001 (see fig. 8). The system has a very high static sensitivity, better than the requested  $3 \text{ phel}/100\text{ns}$ : we got a very low electronic noise of  $\leq 0.5 \text{ phel}/100\text{ns}$  and a noise of about  $1.5 \text{ phel}/100\text{ns}$  with sky-noise background included, see (Gemmeke et al., 2001). But an absolute calibration is still pending. Some work has still to be done to achieve the final trigger threshold under dynamic conditions of read-out. The hardware trigger delivers the expected background suppression of  $5 \cdot 10^9$ . The software triggers are under evaluation.

First cosmic events have been already observed. Fig.9 shows a twenty pixel long cosmic particle with a time length of about  $8 \mu\text{s}$ . From the angular velocity we get in first approximation an event in a distance of 5 km, and from the time length a 2.4 km long track in the field of the telescope.

The second telescope will be installed in July. The final design of the system will be defined in the critical design review in August 2001. The completion of the system with 30 telescopes is planned for end of 2004.

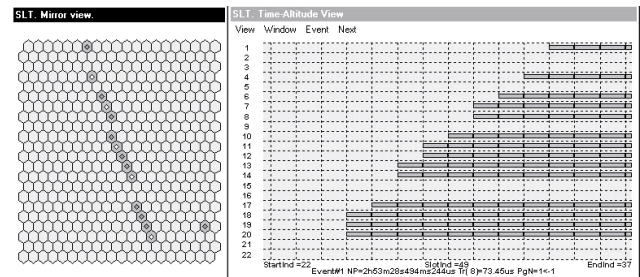


**Fig. 9.** First high energy cosmic particle seen in Malargüe. One time slot corresponds to  $1 \mu\text{s}$ . The mirror inverts the picture. Particles from the sky enter from the bottom of the camera.

## References

- The Pierre Auger Observatory design report, 2nd edition, March 1997, The Auger Collaboration, [www.auger.org/admin](http://www.auger.org/admin).
- Argiro, S. et al., The analog Signal Processor of the Auger Fluorescence Detector Prototype, presented at the Elba meeting on Advanced Detectors 2000, to be published in *NIM*.
- Camin, D. et al., Monitoring DC anode current of a grounded-cathode photomultiplier tube, *NIM A* **435** (1999) 484
- Gemmeke, H. et al., Design of the Trigger System for the Auger Fluorescence Detector, *IEEE-NSS* **47** (2000) 519.
- Gemmeke, H. et al., First Measurements with the Auger Fluorescence Detector data acquisition system, contribution to the ICRC2001 Hamburg.
- Data Sheet of IL300, Infineon 2000, [www.infineon.com/opto](http://www.infineon.com/opto).